A Novel RSPF Approach to Prediction of High-Risk, Low-Probability Failure Events

Marcos E. Orchard[1], Liang Tang[2], Kai Goebel[3], and George Vachtsevanos[2,4]

[1] *Electrical Engineering Department, Universidad de Chile, Santiago 8370451, Chile*
morchard@ing.uchile.cl

[2] *Impact Technologies, LLC, Rochester, NY 14623, USA*
liang.tang@impact-tek.com

[3] *NASA Ames Research Center, MS 269-4, Moffett Field, CA. 94035, USA*
kai.goebel@nasa.gov

[4] *School of Electrical and Computer Engineering, Georgia Institute of Technology, Atlanta, GA 30332, USA*
gjv@ece.gatech.edu

ABSTRACT

Particle filters (PF) have been established as the de facto state of the art in failure prognosis, and particularly in the representation and management of uncertainty in long-term predictions when used in combination with outer feedback correction loops. This paper presents a novel Risk-Sensitive PF (RSPF) framework that complements the benefits of the classic approach, by representing the probability of rare and costly events within the formulation of the nonlinear dynamic equation that describes the evolution of the fault condition in time. The performance of this approach is thoroughly compared using a set of proposed metrics for prognosis results. The scheme is illustrated with real vibration feature data from a fatigue-driven fault in a critical aircraft component.*

1 INTRODUCTION

A number of approaches have been suggested in the recent years for uncertainty representation and management in prediction. In fact, probabilistic, soft computing methods, and tools derived from evidential theory or Dempster-Shafer theory (Shafer, 1976) have been already explored for this purpose. Although probabilistic methods offer a mathematically rigorous methodology, they typically require a statistically sufficient database to estimate the required distributions. Soft-computing methods (fuzzy logic) offer an alternative when scarce data or contradictory data are available. Dempster's rule of combination and such concepts from evidential theory as belief on plausibility (upper and lower bounds of probability) based on mass function calculations can support uncertainty representation and management tasks. Confidence Prediction Neural Networks (NN) (Khiripet, 2001) have also been used to represent and manage uncertainty using Parzen windows as the kernel and a structure based on Specht's General Regression NN (Specht, 1991). Last but not least, probabilistic reliability analysis tools employing an inner-outer loop Bayesian update scheme (Cruse, 2004) have also been used to "tune" model hyper-parameters given observations.

Particle-filtering (PF) based prognostic algorithms (Orchard, 2005; Orchard, 2008; Orchard, 2009; Patrick, 2007; Zhang, 2009) have been established as the de facto *state of the art* in failure prognosis. PF algorithms allow to avoid the assumption of Gaussian (or log-normal) pdf in nonlinear processes, with unknown model parameters, and simultaneously help to consider non-uniform probabilities of failure for particular regions of the state domain. Particularly, the authors in (Orchard, 2008) have proposed a mathematically rigorous method (based on PF, function kernels, and outer correction loops) to represent and manage uncertainty in long-term predictions. However, there are still unsolved issues regarding the proper representation for the probability of rare and costly events, since these events are associated to particles located at the tails of the predicted probability density functions (pdf's).

This paper presents a solution for the aforementioned problem and it is structured as follows. Section 2 introduces the basics of particle filtering (PF) and its application to the field of failure prognostics. Section 3 presents the proposed Risk-Sensitive PF (RSPF) framework and describes implications of the algorithm parameter tuning that has to be considered in the design. Section 4 proposes a set of novel performance metrics to be used in the assessment of prognostic results and evaluates the RSPF, when compared to the classic PF prognosis framework (Orchard, 2009). Section 5 states the most important conclusions.

2 PARTICLE FILTERING AND FAILURE PROGNOSIS

2.1 Risk-Sensitive Particle Filtering

Nonlinear filtering is defined as the process of using noisy observation data to estimate at least the first two moments of a state vector governed by a dynamic nonlinear, non-Gaussian state-space model. From a Bayesian standpoint, a nonlinear filtering procedure intends to generate an estimate of the posterior probability density function $p(x_t \mid y_{1:t})$ for the state, based on the set of received measurements. Particle Filtering (PF) is an algorithm that intends to solve this estimation problem by efficiently selecting a set of N particles $\{x^{(i)}\}_{i=1\cdots N}$ and weights $\{w_t^{(i)}\}_{i=1\cdots N}$, such that the state pdf may be approximated by (Andrieu, 2001; Arulampalam, 2002; Doucet, 1998; Doucet 2001)

$$\begin{aligned} \tilde{\pi}_t^N(x_t) &= \sum_{i=1}^{N} w_t^{(i)} \delta(x_t - x_t^{(i)}) \\ w(x_{0:t}) &= \frac{\pi_t(x_{0:t})}{q_t(x_{0:t})} \propto \frac{p(y_t \mid x_t)\, p(x_t \mid x_{0:t-1})}{q_t(x_t \mid x_{0:t-1})} \end{aligned}, \qquad (1)$$

where $q_t(x_{0:t})$ is referred to as the importance sampling density function (Andrieu, 2001). The choice of this importance density function is critical for the performance of the particle filter scheme. In the particular case of nonlinear state estimation, the value of the particle weights $w_{0:t}^{(i)}$ is computed by setting the importance density function equal to the *a priori* pdf for the state, i.e., $q_t(x_{0:t} \mid x_{0:t-1}) = p(x_t \mid x_{t-1})$ (Arulampalam, 2002). Although this choice of importance density is appropriate to estimate the most likely probability distribution according to a particular set of measurement data, it does not offer a good estimate of the probability of events associated to high-risk conditions with low likelihood.

In this sense, the risk-sensitive particle filter (RSPF) (Thrun , 2001; Verma 2004) incorporates a cost model in the importance distribution to generate more particles in high-risk regions of the state-space. Mathematically, the importance distribution is set as

$$q\left(\tilde{d}_t, \tilde{x}_t \mid \tilde{d}_{0:t-1}^{(i)}, x_{0:t-1}^{(i)}, y_{1:t}\right) = \gamma_t \cdot r(d_t) \cdot p\left(d_t, \tilde{x}_t \mid y_{1:t}\right), \qquad (2)$$

where d_t is a set of discrete-valued states representing fault modes, x_t is a set of continuous-valued states that describe the evolution of the system given those operating conditions, $r(d_t)$ is a positive risk function that is dependent on the fault mode, and γ_t is a normalizing constant. This methodology has proven to be very helpful in FDI applications, improving the tracking of states that are critical to the performance of a six-wheel robot (Verma 2004), although no applications in the prognostic arena have been published so far. It is important to note, though, that this PF approach needs the inclusion of exogenous models to evaluate and estimate the risk associated with every fault mode, a task that may prove to be difficult to implement in absence of expert opinions.

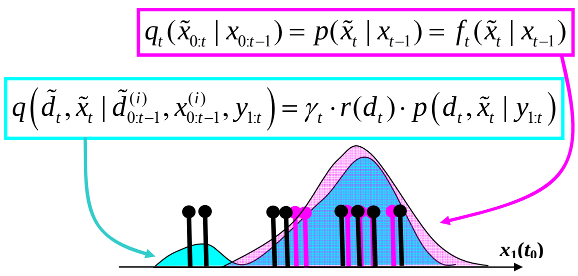

Figure 1: Particle population using either the a priori state pdf or a risk-sensitive pdf as importance distribution for $x_1(t)$

The RSPF-based approach for failure prognosis presented in this paper ensures the existence of particles in the tails of the state pdf to represent the probability of events associated to high-risk conditions with low likelihood, which in practice implies a more conservative estimate of the remaining useful life (RUL) of a piece of equipment. The weights of the particles located at the tails of the pdf (which are updated each time a new measurement is obtained) represent an estimate of the mass probability of the tails, i.e., particles in the regions of the state space that are believed to have low likelihood; see Fig. 1. In situations where effectively the data shows no signs of this critical type of events, the weights of these particles should decrease over time. Nevertheless, the information provided by these weights is of paramount importance, since it allows considering catastrophic events in the schedule of the system operation and enables fast adjustments in prognosis results in the presence of incipient critical conditions (Orchard, 2009).

2.2 Failure Prognosis using Particle Filters

Prognosis, and thus the generation of long-term prediction, is a problem that goes beyond the scope of filtering applications since it involves future time horizons. Hence, if PF-based algorithms are to be used, it is necessary to propose a procedure with the capability to project the current particle population in time in the absence of new observations (Orchard, 2009).

Any adaptive prognosis scheme requires the existence of at least one feature providing a measure of the severity of the fault condition under analysis (fault dimension). If many features are available, they can always be combined to generate a single signal. In this sense, it is always possible to describe the evolution in time of the fault dimension through the nonlinear state equation (Orchard, 2008):

$$\begin{cases} x_1(t+1) = x_1(t) + x_2(t) \cdot F(x(t),t,U) + \omega_1(t) \\ x_2(t+1) = x_2(t) + \omega_2(t) \end{cases}, \tag{3}$$

where $x_1(t)$ is a state representing the fault dimension under analysis, $x_2(t)$ is a state associated with an unknown model parameter, U are external inputs to the system (load profile, etc.), $F(x(t),t,U)$ is a general time-varying nonlinear function, and $\omega_1(t)$, $\omega_2(t)$ are white noises (not necessarily Gaussian). The nonlinear function $F(x(t),t,U)$ may represent a model based on first principles, a neural network, or even a fuzzy system.

By using the aforementioned state equation to represent the evolution of the fault dimension in time, it is possible to generate long term predictions using kernel functions to reconstruct the estimate of the state pdf in future time instants:

$$\hat{p}(x_{t+k} \mid \hat{x}_{1:t+k-1}) \approx \sum_{i=1}^{N} w_{t+k-1}^{(i)} K\left(x_{t+k} - E\left[x_{t+k}^{(i)} \mid \hat{x}_{t+k-1}^{(i)}\right]\right), \tag{4}$$

where $K(\cdot)$ is a kernel density function, which may correspond to the process noise pdf, a Gaussian kernel or a rescaled version of the Epanechnikov kernel (Orchard, 2008).

The resulting predicted state pdf contains critical information about the evolution of the fault dimension over time. One way to represent that information is through the computation of statistics (expectations, 95% confidence intervals), either the Time-of-Failure (ToF) or the Remaining Useful Life (RUL) of the faulty system. A detailed procedure to obtain the RUL pdf from the predicted path of the state pdf is described and discussed in (Orchard, 2009), although the general concept is as follows. Basically, the RUL pdf can be computed from the function of probability of failure at future time instants. This probability is calculated using both the long-term predictions and empirical knowledge about critical conditions for the system. This empirical knowledge is usually incorporated in the form of thresholds for main fault indicators, also referred to as the hazard zones.

In real applications, it is expected for the hazard zones to be statistically determined on the basis of historical failure data, defining a critical pdf with lower and upper bounds for the fault indicator (H_{lb} and H_{ub}, respectively). Since the hazard zone specifies the probability of failure for a fixed value of the fault indicator, and the weights $\left\{w_{t+k}^{(i)}\right\}_{i=1\cdots N}$ represent the predicted probability for the set of predicted paths, then it is possible to compute the probability of failure at any future time instant (namely the RUL pdf) by applying the law of total probabilities, as shown in Eq. (5). Once the RUL pdf is computed, combining the weights of predicted trajectories with the hazard zone specifications, it is well known how to obtain prognosis confidence intervals, as well as the RUL expectation.

$$\hat{p}_{TTF}(t) = \sum_{i=1}^{N} \Pr\left(Failure \mid X = \hat{x}_t^{(i)}, H_{lb}, H_{ub}\right) \cdot w_t^{(i)} \tag{5}$$

3 RSPF-BASED PROGNOSTIC FRAMEWORK, CASE STUDY AND ANALYSIS OF RESULTS

A RSPF-based approach for failure prognosis intends to represent the probability of rare and costly events within the formulation of the nonlinear dynamic equation describing the evolution of the fault condition in time, and thus modifying the Time-of-Failure (ToF) pdf estimate accordingly. In particular, it is proposed to implement a variant of this RSPF algorithm where the cost function in Eq. (2) allows sampling particles $x^{(i)}(t)$ ($i = 1 \ldots N_r$, $N_r << N$), using the nonlinear model in Eq. (3), from regions of the state space where $x_1^{(i)}(t)$ has low likelihood. This ensures the existence of particles in the tails of the state pdf that represent the probability of events associated to high-risk conditions with low likelihood.

The RSPF-based algorithm is implemented here by modifying the kernel of the noise $\omega_1(t)$ in Eq. (3), and thus allowing some particles to be created in regions of the state space that represent extreme and rare changes in the evolution of the fault condition. In practice, this kernel modification implies a more conservative estimate of the remaining useful life (RUL). The weights of the particles located at the tails of the original noise pdf represent an estimate of the mass probability of the tails and are updated accordingly to the new measurements. Information provided by these weights allows considering the probability of a catastrophic event and enables adjustments in prognosis results in the presence of incipient critical conditions

A test case has been designed to evaluate the performance of a RSPF-based prognostic framework and to analyze the main aspects of algorithm implementation that help to improve online state estimates. Consider the case of propagating fatigue crack on a critical component in a rotorcraft transmission system. The objective in this seeded fault test is to analyze how a cyclic load profile affects the growth of an axial crack. Although the physics-based model for a system of these characteristics may be complex, it is possible to represent the growth of the crack (fault dimension) using the much simpler population-growth-based model (Orchard, 2008):

$$\begin{cases} x_1(t+1) = x_1(t) + C \cdot x_2(t) \cdot (a - b \cdot t + t^2)^m + \omega_1(t) \\ x_2(t+1) = x_2(t) + \omega_2(t) \end{cases}, \quad (6)$$

where $x_1(t)$ is a state representing the fault dimension, $x_2(t)$ is a state associated with an unknown model parameter, C and m are constants associated with the fatigue properties of the material. The constants a and b depend on the maximum load and duration of the load cycle (external input U). Given a set of vibration feature data such as described in (Orchard, 2008; Orchard, 2009, Patrick, 2007), it is possible to use this model to obtain an approximate (and noisy) estimate of the crack length via the use of a PF-based algorithm (Orchard, 2009). Once the estimate of the state pdf is available, it can be used as initial condition of the model to generate long-term predictions, if the integrals in the aforementioned recursive expression are evaluated.

The evolution in time of the fault dimension is described by Eq. (6), where $\omega_1(t)$ is white noise distributing as a Gaussian mixture; i.e., the distribution of the process noise $\omega_1(t)$ can be written as:

$$\omega_1(t) \sim \ \delta \cdot \omega_1'(t) + (1-\delta) \cdot \omega_1^*(t), \quad (7)$$

where $0 \leq \delta \leq 1$, $\omega_1'(t) \sim N(0, \sigma'^2)$, $d = E\left\{\omega_1^*(t)\right\} \neq 0$, and $\omega_1^*(t) \sim N(d, \sigma^{*2})$.

Consequently, RSPF-based prognostic algorithms have three extra parameters to be defined, compared with classic PF-based implementations. However, if the variance of the Gaussian kernels are selected in such a way that $\sigma' = \sigma^*$ and equal to the process noise variance of the classic PF approach, then only d and δ must be considered as extra design parameters.

In the test case used for the analysis, feature data associated to the fault is fed into the RSPF-based prognostic algorithm to estimate the ToF pdf. Arbitrary initial conditions are set for the unknown model parameter in Eq. (6), and it is known that failure mechanisms may undergo changes after the 400th cycle of operation due to the size of the fault. Result analysis will focus on the quality of the estimate for the unknown model parameter, $E\left[x_2(t)\right]$, after the 400th cycle of operation and on the accuracy exhibited by the corresponding ToF pdf estimate. Performance comparison is done with respect to a classic (SIR) PF-based prognostic framework (Orchard, 2009), given same initial conditions at time $t = 400$. It must be noted that this implementation considers a correction loop that simultaneously updates the variance of kernel associated to the white noise $\omega_2(t)$ according to the short-term prediction (Orchard, 2008).

Three qualitative aspects are considered in the analysis:

1. Effect of parameter d in online state estimates
2. Effect of parameter δ in the aforementioned estimates
3. Effect of parameter d in ToF pdf estimates

3.1 Effect of parameter "*d*" in online state estimates

Figures 2 and 3 show a comparison of estimation results when using values of d (i.e., $E\{\omega_1^*\}$) selected from the set {0.00, 0.10}. Before commenting these outcomes, it is important to mention that higher absolute values of d imply that the risk-sensitive approach draws particles far away from the most likely range, according to the received measurements. Consequently, the approach will become more sensitive to the appearance of sudden changes in the dynamic of the system, at the price of a possible bias in the estimate.

Indeed, from Fig. 2, there exists a bias in the estimate of the fault dimension when $d = 0.10$ (magenta line in the first plot) that will affect the estimate of the ToF pdf, although there is a compensation effect that translates into a decrement in the value of the unknown model parameter estimate (magenta line in Fig. 3) that diminishes the impact on the resulting ToF pdf estimate. This biased estimate, though, allows the algorithm to quickly react in the presence of changes in operation conditions: the fault dimension estimate is much more accurate between the 420th - 450th cycles of operation, helping the adjustment of the ToF estimate during that time period.

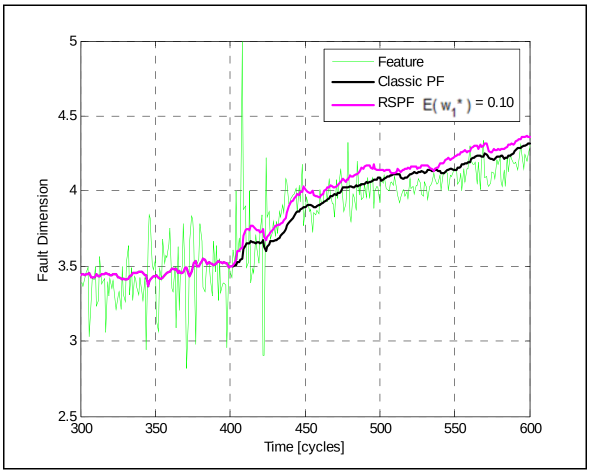

Figure 2: RSPF-based state estimation, $E\{\omega_1^*\} = 0.10$

From Fig. 3, it can be stated the existence of this bias basically forces the estimate of $x_2(t)$ to absorb any inconsistencies in the *a posteriori* state estimate. On top of that, the weight of particles associated to areas of the domain with low likelihood are very small and therefore the algorithm loses its capability to react (in the event of sudden changes in operational conditions) using those particles. Thus, it is recommended for the design to consider an absolute maximum value for the parameter *d* no bigger than $3\sigma'$.

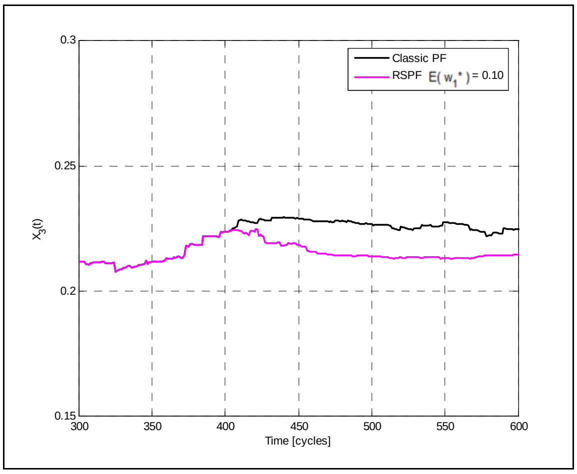

Figure 3: RSPF-based parameter estimate, E{ω1*}=0.10

3.2 Effect of parameter "δ" in online state estimates

Following the same methodology, a test was performed considering two values for δ the parameter associated to the weight of the risk-sensitive kernel ω_1^*. Fig. 4 and 5 illustrate the obtained results. It is clear that the bigger the weight of the risk-sensitive kernel, the stronger is the adjustment made by the algorithm in the estimate of the unknown model parameter. Regarding ToF estimates, it is also clear that these adjustments go in a conservative direction, forcing the ToF pdf estimate to be on the "safer" side (ToF estimate smaller that actual failure time). Conversely, the bigger the value of δ, the more particles will be drawn for areas representing sudden and unexpected changes in operational conditions. Hence, there is an explicit relationship between how conservative the design is, in terms of the ToF estimate, and how sensitive the algorithm is to detect abnormal conditions in the evolution of the fault condition. The more conservative, the more sensitive is the algorithm.

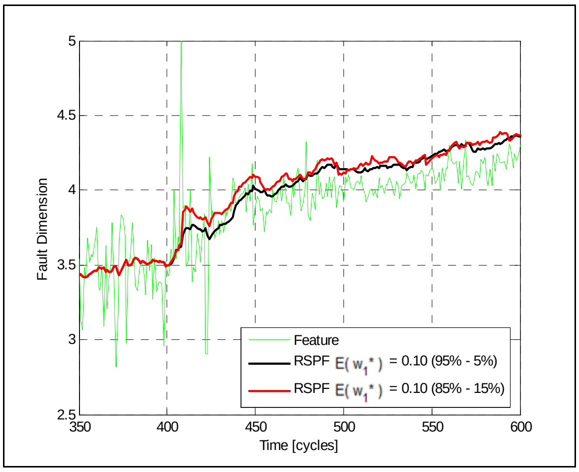

Figure 4: RSPF-based state estimation, δ= 0.05 vs. δ= 0.15

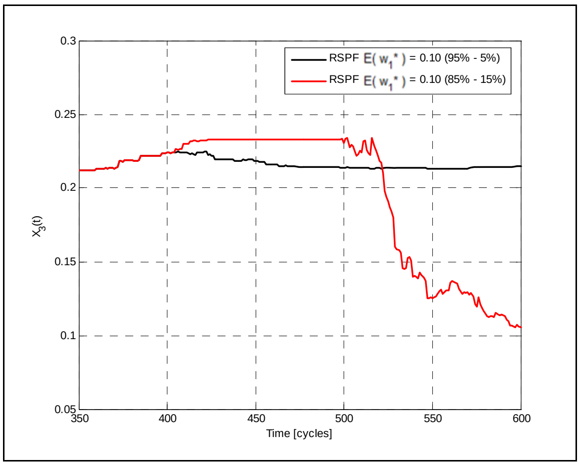

Figure 5: RSPF-based parameter estimate, δ= {0.05, 0.15}

3.3 Effect of parameter "*d*" in ToF estimates

Conclusions stated in Section 3.2 are reinforced when analyzing the results in terms of the ToF pdf estimate that is computed (at the 600th cycle) on the basis of the online PF-based state estimate; see Fig. 6, where the vertical line indicates the ground truth failure time. Indeed, larger values of $d = E\{\omega_1^*\}$ are associated to more conservative estimates for the most likely ToF pdf, given the measured data. Thus, it is an essential part of the design process to define the maximum acceptable bias that is needed to include tails of the probability density function that do not necessarily maximize the likelihood of observations. As a separate note, it is important to mention that the amount of processed data is directly related to the precision of the pdf estimate regardless of the utilized PF approach; see Fig. 7 where the magenta pdf considers data from the 0th cycle, being more precise that the cyan pdf that only considered data from the 400th cycle of operation.

4 PERFORMANCE METRICS AND ASSESSMENT OF RSPF-BASED PROGNOSTIC ALGORITHMS

The estimate obtained from a Particle Filtering algorithm is based on a realization of the stochastic process that is associated to the measurement data. In addition, the generation of the particle population involves sampling procedures that consider a proposed *importance distribution*. In this sense, it is important to mention that the assessment or the comparison between different uncertainty management strategies should consider statistics for the evaluation of a particular performance metric. In the absence of different sets of measurement data, at the least it is recommended to evaluate several realizations of the particle filter algorithm, calculating the mean and standard deviation of the resulting performance metric values.

In general, indices used as performance metrics for prognosis purposes should be capable of representing and evaluating the concepts of "accuracy" and "precision" of the RUL pdf estimate (Vachtsevanos, 2006). "Accuracy" is intimately related to the difference between the actual failure time and the estimate of its expectation, while "precision" is associated to its variance (or standard deviation).

The following proposed indicators intend to help in the assessment of the algorithm effectiveness over time, given a realization of the stochastic process. Since a measure of "accuracy" needs the knowledge of the ground truth failure time, which is unknown before the actual failure in any on-line implementation of prognostic routines, it is proposed to consider the concept of "steadiness" of the RUL estimate instead. The aforementioned indicators must also consider the fact that both the *RUL* and $E_t\{RUL\}$ (estimate, at time *t*, of the expectation of the equipment RUL) are random variables. Moreover, it is assumed that at any current time *t* it is possible to compute an estimate of the 95% confidence interval for the time-of-failure (CI_t), also referred to as the end-of-life (EOL).

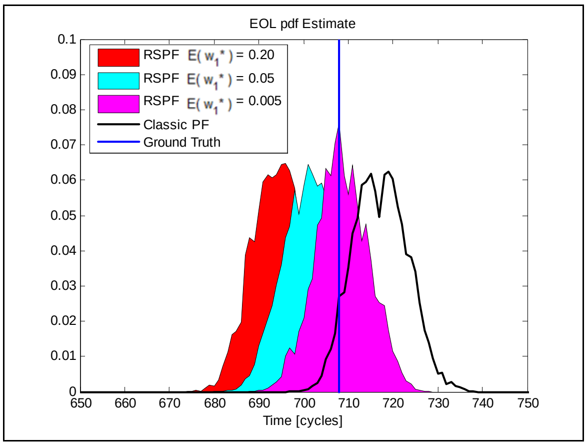

Figure 6: RSPF-based EOL estimate. $E\{\omega_1^*\} = \{0.005, 0.05, 0.20\}$

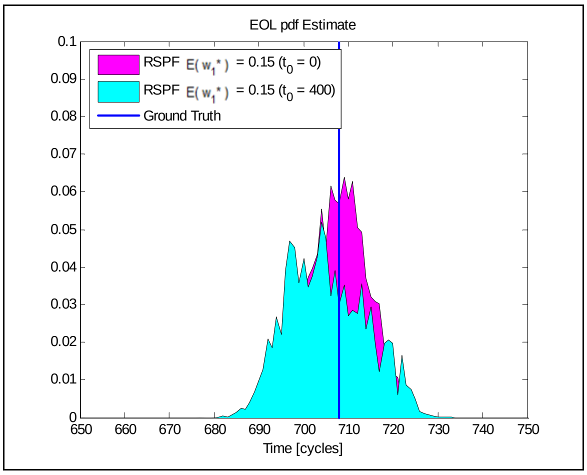

Figure 7: RSPF-based EOL estimate, $t_0 = \{0, 400\}$

4.1 RUL On-line Precision Index (RUL-OPI)

Considers the relative length of the 95% confidence interval computed at time *t* (CI_t), when compared to the remaining useful life. It quantifies the concept: "the more data the algorithm processes, the more precise should the prognostic result be". Good prognostic results present values of $I_1 \approx 1$.

$$I_1(t) = e^{-\left(\frac{\sup(CI_t)-\inf(CI_t)}{E_t\{RUL\}}\right)} = e^{-\left(\frac{\sup(CI_t)-\inf(CI_t)}{E_t\{ToF\}-t}\right)} \tag{8}$$
$$0 < I_1(t) \le 1, \forall t \in [1, E_t\{ToF\}), t \in \mathbb{N}$$

Results of the evaluation of the RUL-OPI index are shown in Fig. 8. The RUL-OPI index strongly penalizes the width of the 95% confidence interval as the number of cycles associated to the fault condition increases. It is interesting to note that the implementation of a RSPF-based approach does not dramatically affect the precision of the obtained confidence interval.

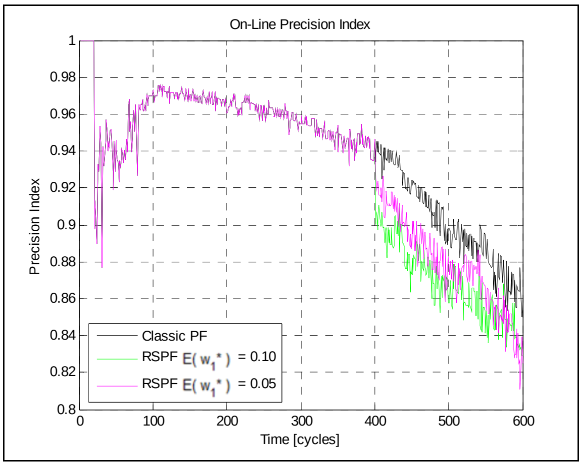

Figure 8: RSPF-based prognostic algorithm. RUL-OPI index

From obtained results it can be stated that the overall effect of RS approaches in algorithm precision is not significant; moreover, precision differences obtained near the end of the analysis (600th operating cycle) are negligible. In this sense, the aggregated value of implementing risk-sensitive techniques exceeds the associated costs.

4.2 RUL Accuracy-Precision Index

It represents the error of *ToF* estimates relative to the width of the corresponding 95% confidence interval CI_t, penalizing whenever the expected ToF $E_t\{\text{ToF}\} > GroundTruth\{\text{ToF}\}$ (actual failure happened before the expected time). Accurate prognostic results are associated to values of the index such that $0 \leq 1 - I_2(t) \leq \varepsilon$, where ε is a small positive constant.

$$I_2(t) = e^{-\left(\frac{Ground\,Truth\{ToF\} - E_t\{ToF\}}{\sup(CI_t) - \inf(CI_t)}\right)} \qquad (9)$$
$$0 < I_2(t), \forall t \in [1, E_t\{ToF\}), t \in \mathbb{N}$$

The effect of implementing RSPF-based approaches is more noticeable when measuring the accuracy of the resulting ToF estimates. In fact, the proposed accuracy metric strongly penalizes estimates that are beyond the ground truth failure time and therefore conservative approaches (such as RSPF) are better evaluated than more aggressive ones. In general, the bias introduced in the state estimation procedure reflects itself in low values of the accuracy-precision index, although accuracy improves as more data comes into analysis. Again, the design question that must be answered is: how conservative must the approach be? More conservative approaches will affect the overall accuracy, but will have more sensitivity to abrupt (and dangerous) changes in the failure dynamics or operating conditions. It is important to mention that the proposed restriction for the parameter *d* of the algorithm helps to narrow the effect on accuracy performance.

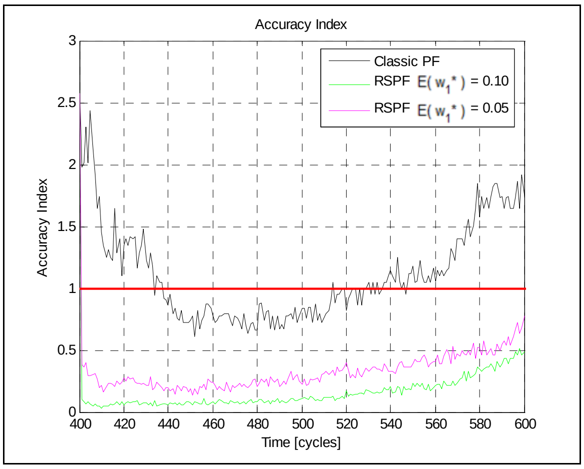

Figure 9: RSPF-based prognostic algorithm. RUL accuracy-precision index

4.3 RUL On-line Steadiness Index (RUL-OSI)

This indicator considers the quality of the current ToF expectation, which is computed given measurement data available at time *t*. It quantifies the concept: "the more data the algorithm processes, the steadier the prognostic result" Good prognostic results are associated to small values for the RUL-OSI.

$$I_3(t) = \sqrt{Var\left(E_t\{ToF\}\right)} \qquad (10)$$
$$I_3(t) \geq 0, \forall t \in \mathbb{N}$$

The analysis of the steadiness index has special meaning when is performed on a sliding window, since it also allows to keep track of the effect of outer correction loops in the prognostic framework. Results of this analysis are shown in Fig. 10, considering a sliding window of 40 samples to compute the value of the RUL-OSI index. It must be noted that the steadiness index with sliding window shows similar results for all approaches, which basically indicates that prognostic results have similar ranges for the updates performed on the ToF pdf estimates over the time period represented by the sliding window. Increments in the value of this index are typically associated to the activation of outer correction loops, since strong updates in the unknown model parameter estimate will affect the ToF estimate similarly.

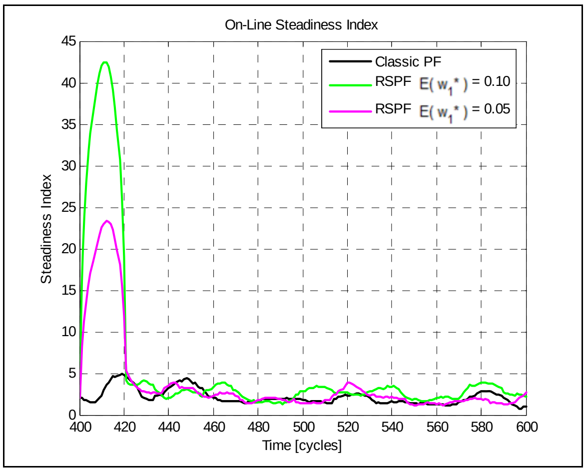

Figure 10: RSPF-based prognostic algorithm. RUL-OSI (steadiness) index

5 CONCLUSION

This paper presents a novel RSPF-based prognostic framework that helps to represent the probability of rare and costly events in the evolution of the fault condition in time. A detailed performance analysis, using a set of proposed metrics for prognostics, shows that the presented approach ensures the existence of particles in the tails of the state pdf, generally providing a more conservative estimate of the remaining useful life (RUL) of the faulty piece of equipment. In addition, it has been shown that precision and steadiness of the prognostic result is not affected significantly, although it is recommended to activate the RSPF-based framework in a secondary stage, once the classic PF state estimate has shown adequate steadiness (generally after the reaction of outer correction loops). The scheme is illustrated with real vibration feature data from a fatigue-driven fault in a critical aircraft component.

ACKNOWLEDGMENT

The authors would like to acknowledge and thank NASA Ames for supporting research in the area of prognostic uncertainty management, Dr. Johan Reimann and Dr. Gregory Kacprzynski of Impact Technologies, and for Dr. Orchard's financial support from Conicyt via Fondecyt #11070022.

REFERENCES

(Andrieu, 2001) C. Andrieu, A. Doucet, and E. Punskaya, “Sequential Monte Carlo Methods for Optimal Filtering,” in *Sequential Monte Carlo Methods in Practice*, A. Doucet, N. de Freitas, and N. Gordon, Eds. NY: Springer-Verlag, 2001.

(Arulampalam , 2002) M.S. Arulampalam, S. Maskell, N. Gordon, and T. Clapp, “A Tutorial on Particle Filters for Online Nonlinear/Non-Gaussian Bayesian Tracking,” *IEEE Transactions on Signal Processing*, vol. 50, no. 2, Feb. 2002, pp. 174 – 188.

(Cruse, 2004) T.A. Cruse, “*Probabilistic Systems Modeling and Validation*,” HCF 2004, March 16-18, 2004.

(Doucet, 1998) A. Doucet, “On sequential Monte Carlo methods for Bayesian Filtering,” Technical Report, Engineering Department, Univ. Cambridge, UK, 1998.

(Doucet, 2001) A. Doucet, N. de Freitas, and N. Gordon, “An introduction to Sequential Monte Carlo methods,” in *Sequential Monte Carlo Methods in Practice*, A. Doucet, N. de Freitas, and N. Gordon, Eds. NY: Springer-Verlag, 2001.

(Khiripet, 2001) N. Khiripet, G. Vachtsevanos, A. Thakker, and T. Galie, “A New Confidence Prediction Neural Network for Machine Failure Prognosis”, *Proceedings of Intelligent Ships Symposium IV*, Philadelphia, PA, April 2-3, 2001.

(Orchard, 2005) M. Orchard, B. Wu, and G. Vachtsevanos, “A Particle Filter Framework for Failure Prognosis”, *Proceedings of World Tribology Congress III*, Washington DC, Sept. 12-16, 2005.

(Orchard, 2008) M. Orchard, G. Kacprzynski, K. Goebel, B. Saha, and G. Vachtsevanos, “Advances in Uncertainty Representation and Management for Particle Filtering Applied to Prognostics,” 2008 *International Conference on Prognostics and Health Management* PHM 2008, Denver, CO, USA, October 9 – 12, 2008.

(Orchard, 2009) M. Orchard, *On-line Fault Diagnosis and Failure Prognosis Using Particle Filters. Theoretical Framework and Case Studies*, Publisher: VDM Verlag Dr. Müller Aktiengesellschaft & Co. KG, Saarbrücken, Germany, April 2009, 108 pages. Atlanta: The Georgia Institute of Technology, Diss., 2007.

(Patrick, 2007) R. Patrick, M. Orchard, B. Zhang, M. Koelemay, G. Kacprzynski, A. Ferri, and G. Vachtsevanos, “An Integrated Approach to Helicopter Planetary Gear Fault Diagnosis and Failure Prognosis,” 42nd Annual Systems Readiness Technology Conference, AUTOTESTCON 2007, Baltimore, USA, September 2007.

(Shafer, 1976) G. Shafer, *A mathematical theory of evidence*, Princeton, N.J: Princeton University Press, 1976.

(Specht, 1991) D.F. Specht, “A General Regression Neural Network”, *IEEE Trans on Neural Networks*, vol. 2, no. 6, pp. 568-76, Nov, 1991.

(Thrun, 2001) S. Thrun, J. Langford, and V. Verma, “Risk Sensitive Particle Filters,” Neural Information Processing Systems (NIPS), Dec. 2001.

(Verma, 2004) V. Verma, G. Gordon, R. Simmons, and S. Thrun, “Particle Filters for Rover Fault Diagnosis,” *IEEE Robotics & Automation Magazine*, pp. 56 – 64, June 2004.

(Vachtsevanos, 2006) G. Vachtsevanos, F.L. Lewis, M.J. Roemer, A. Hess, and B. Wu, *Intelligent Fault Diagnosis and Prognosis for Engineering Systems*, Hoboken, NJ, John Wiley and Sons, 2006.

(Zhang, 2009) B. Zhang, T. Khawaja, R. Patrick, M. Orchard, A. Saxena, and G. Vachtsevanos, “A Novel Blind Deconvolution De-Noising Scheme in Failure Prognosis,” *IEEE Transactions on Instrumentation and Measurement*, vol. 58, no. 2, pp. 303-310, February 2009.